ORGANIC PROCESS RESEARCH & DEVELOPMENT
OPR&D

Full Paper

Development and Scaling-Up of the Fragrance Compound 4-Ethylguaiacol Synthesis via a Two-Step Chemo-Enzymatic Reaction Sequence

Lorenzo Pesci, Maik Baydar, Silvia Glueck, Kurt Faber, Andreas Liese, and Selin Kara

Org. Process Res. Dev., **Just Accepted Manuscript** • DOI: 10.1021/acs.oprd.6b00362 • Publication Date (Web): 02 Dec 2016

Just Accepted

ACS Publications

Organic Process Research & Development is published by the American Chemical Society. 1155 Sixteenth Street N.W., Washington, DC 20036

Development and Scaling-Up of the Fragrance Compound 4-Ethylguaiacol Synthesis *via* a Two-Step Chemo-Enzymatic Reaction Sequence

Lorenzo Pesci,[†] *Maik Baydar,* [†] *Silvia Glueck,*[‡,§] *Kurt Faber,*[‡]

Andreas Liese *[†] *and Selin Kara* *[†]

[†] Institute of Technical Biocatalysis, Hamburg University of Technology, Denickestr. 15, 21073 Hamburg (Germany)

[‡]ACIB GmbH, Petersgasse 14, 8010 Graz (Austria)

[§]Department of Chemistry, Organic & Bioorganic Chemistry, University of Graz, Heinrichstrasse 28, 8010 Graz (Austria)

ABSTRACT

The transformation of (abundant) oxygenated biomass-derived building blocks *via* chemo-enzymatic methods is a valuable concept for accessing useful compounds, as it combines the high selectivity of enzymes and the versatility of chemical catalysts. In this work, we demonstrate a straightforward combination of a phenolic acid decarboxylase (PAD) and palladium on charcoal (Pd/C) that affords the flavor compound 4-ethylguaiacol from ferulic acid. The use of a two-phase system proved advantageous in terms of enzyme activity, stability, and volumetric productivity, and allows to carry out the hydrogenation step directly in the organic layer containing exclusively the intermediate, 4-vinylguiacol. The enzymatic decarboxylation step in the biphasic system afforded 89% conversion of 100 mM (19 g L^{-1}) ferulic acid with an isolated yield of 75%. By extracting 4-vinylguiacol continuously into the organic phase, conversion was enhanced to 92% using 170 mM (33 g L^{-1}) ferulic acid, which was only possible in the continuous extraction and distillation set-up developed. The reaction cascade (PAD–Pd/C) is demonstrated at gram scale, affording the target product 4-ethylguaiacol (1.1 g) in 70% isolated yield in a two-steps two-pots process. The enzymatic step was characterized in detail to overcome major constraints and the process favorably compares in terms of the environmental impact with traditional approaches.

KEYWORDS: Biocatalysis, Decarboxylation, Chemical Reduction, Chemo-Enzymatic Cascade, Biphasic System

INTRODUCTION

The combination of enzymatic and – especially heterogeneous – chemical catalysis has been addressed as a promising concept for the realization of sequential conversions of renewable feedstocks.[1] This is in part due to the synergic effect arising from the high selectivity offered by homogeneously solubilized enzymes and the robustness of heterogeneous chemical catalysts. In this context, Pd-catalyzed reductions were employed in cascade reactions partnered by enzymes in either "one-pot" or "two-pots" fashion.

Recent examples include (i) the *in situ* generation of H_2O_2 for chloroperoxidase-catalyzed oxidation of anisole,[2] (ii) the diastereoselective reduction of Δ^1-2,6-disubstituted piperidines obtained from a transaminase reaction,[3] (iii) the alcohol dehydrogenase-Pd catalyzed carbonyl and azide reductions to access β-amino alcohols,[4] (iv) the routes to (*R*)-2-acetoxy-1-indanol *via* regioselective chemical hydrogenation coupled with chemoenzymatic dynamic kinetic resolution[5] and (v) to (*S*)-γ-hydroxymethyl-α,β-butenolide *via* chemical hydrogenation and lipase-mediated Baeyer–Villiger oxidation starting from cellulose-derived levoglucosenone.[6]

Alkyl and vinyl phenols are aroma compounds present in different types of foods and beverages. For example, 4-ethylguaiacol (4-EG) is present in cooked asparagus, raw Arabica coffee beans, scotch whiskey and tequila as well as in soy sauce, while 4-vinylguaiacol (4-VG) contributes to the aroma of beer, tortilla chips, rice bran and raw Arabica coffee beans as well.[7] As these compounds are FDA-approved flavouring agents,[8] their synthesis is of a high industrial interest.

Scheme 1 depicts a retrosynthetic analysis involving chemical and enzymatic methods to access 4-VG and 4-EG starting from the guaiacol scaffold 2-methoxyphenol. Route 1 to 4-EG *via* Friedel–Crafts alkylation is probably the least desirable, as recent studies using acid catalysts

reveal competition between C- and O-alkylation and incomplete regioselectivity in the C-alkylation due to the presence of the phenol and methoxy groups.[9] Route 2 is selective, but involves the use of amalgamated Zn in stoichiometric amounts.[10] A recently developed alternative is the Cu-doped porous metal oxide-catalyzed hydrogenolysis in methanol at 0.3 mol% catalyst loading at H_2 pressure (40 bar) and 180°C.[11] Mild hydrogenation conditions can be applied using palladium on charcoal (Pd/C) catalysis (route 6). 4-VG can be synthesized starting from the corresponding aldehyde (route 3) in a Knoevenagel–Doebner condensation using malonic acid and piperidine as organocatalyst[12] in pyridine,[13] or by Wittig olefination.[14] Heck cross-coupling using aryl bromides (route 4) at low ethylene pressure can only be used if the phenolic hydroxyl group is protected.[15] Alternatives are the Pd-catalyzed cross-coupling using vinyl Grignard reagents[16] or Stille coupling.[17]

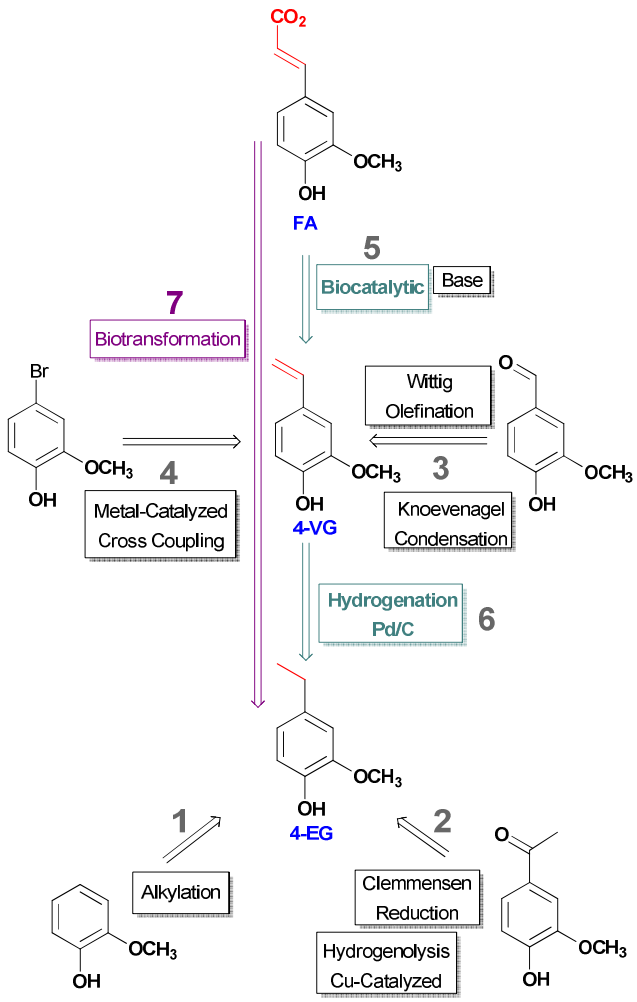

Scheme 1. Retrosynthetic analysis for 4-vinylguaiacol (4-VG) and 4-ethylguaiacol (4-EG).

Alternatively, 4-VG can be obtained by decarboxylation of ferulic acid (FA) (route 5). This reaction can be performed chemically by treating FA with base at elevated temperature (inorganic base in refluxing DMF,[18] DBU or $NaHCO_3$/[Hmim]Br under microwave irradiation.[19,20] A milder method of obtaining 4-VG is the biocatalytic variant using phenolic acid decarboxylases (PADs, EC 4.1.1.–). FA is abundantly available from lignocellulosic biomass[21] and constitutes an ideal platform for the synthesis of functionalized aromatics, such as vanillin.[22] Although fermentation protocols using either wild-type fungal strains (*Candida* and *Aspergillus*)[23,24,25] or engineered *E. coli*[26] yielding 4-VG and 4-EG from FA were established

(route 7), these *in vivo* strategy yields in general low productivities due to limited substrate (FA) concentrations. Alternatively, 4-VG can also be reduced enzymatically by NADH-dependent vinyl phenol reductases.[27,22]

Our study focused on routes 5 and 6 by combination of biocatalytic decarboxylation of 4-hydroxycinnamic acids by PADs yielding 4-hydroxystyrenes, followed by Pd-catalyzed hydrogenation of the vinyl bond without intermediate isolation. Regarding the first step, PADs, first characterized in the 1990s from *Bacillus* and *Lactobacillus*[28,29] sources, have received increasing attention during the last years in view of the (industrial) production of bio-based styrene polymers.[30,31,32] Two-phase systems are used to run biotransformations at high substrate concentrations[33], as also shown for this reaction.[33a]

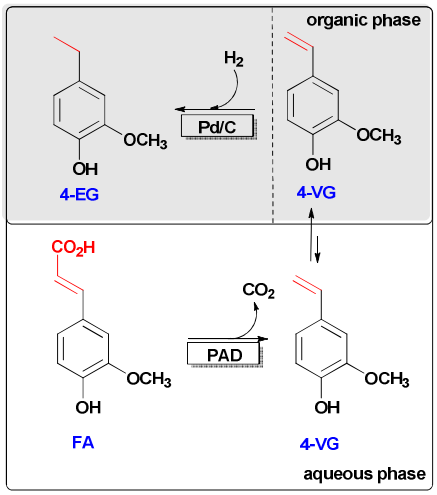

Scheme 2. Reaction sequence of PAD-catalyzed decarboxylation of FA and subsequent hydrogenation catalyzed by Pd/C in the organic phase. The dashed line indicates that the hydrogenation reaction in organic phase takes place subsequently in a second reactor.

In this work, we carried out a detailed investigation of the biocatalytic decarboxylation of FA catalyzed by PAD from *Mycobacterium colombiense* (*Mc*PAD, not studied for this purpose so far) in one- and two-liquid phase (2LPS) systems, including a mathematical modelling of the reaction. Under optimized conditions in a 2LPS, the organic layer containing the intermediate 4-VG could be easily transferred to the hydrogenation reactor yielding 4-EG (Scheme 2).

RESULTS AND DISCUSSION

Enzyme Characterization, Kinetics and Simulation

Our initial experiments on the characterization of the *Mycobacterium colombiense* PAD (*Mc*PAD) regarding pH and temperature showed that maximum values in terms of activity and conversion are at pH 6–7 (potassium phosphate (KPi) buffer, ESI Figure S1), which is similar to that of PADs from bacteria and from yeast. [33-36] Regarding the temperature, the activity increased between 20 and 50°C (Figure S2), however, quantitative conversions were achieved only between 20 and 37°C due limited enzyme stability ($t_{1/2}$ ~1 h at 50°C). For further studies, we chose KP_i buffer at pH 7.0 and 37°C (40% residual activity after 24 h, ESI Figure S2). With respect to the kinetics, a typical saturation curve was fitted using the single-substrate Michaelis–Menten equation (ESI Figure S3 and S4). Kinetic parameters with standard deviation for *Mc*PAD-catalyzed decarboxylation of ferulic acid (FA) were found as: $K_{M,FA}$ 2.4 ± 0.1 mM, V_{max} 90 ± 1 U mg^{-1}, and $K_{i,4-VG}$ 0.14 ± 0.04 mM.

In comparison to other PADs, the K_M values are all in the same range (usually between 0.8 and 2 mM, in general <10 mM). For example, K_M values for PADs from *Candida guillermondi*, *Bacillus subtilis*, *Enterobacter* sp., *Lactobacillus brevis* and *Saccharomyces cerevisiae* are 5.3 mM,[37] 1.1 mM,[38] 2.4 mM,[39] 0.96 mM,[35] and 0.79 mM[36] for their phenolic substrates,

respectively. On the other hand, V_{max} values are more diverse: the PAD from yeast has a value of 6.8×10^{-3} U mg^{-1}), the one from *C. guillermondi* 378 U mg^{-1} and the enzyme from *L. brevis* 10 U mg^{-1}.

Next, we determined product inhibition for *Mc*PAD by measuring initial rates in the presence of increasing product (4-VG) concentrations (ESI Figure S5). Assuming a mechanism involving competitive product inhibition (i.e. the product binds reversibly to the enzyme forming an enzyme-product complex which impedes substrate binding), we fitted the progresses of batch reactions to Equation 1 (Eqn. 1) by regression of the inhibition constant $K_{i,4-VG}$. The equation represents the proposed catalytic mechanism, where [PAD] is the enzyme concentration, [FA] and [4-VG] are the concentrations of substrate and product.

$$v = \frac{V_{max}\,[FA]}{K_{M,FA}\,(1+\frac{[4-VG]}{K_{i,4-VG}})+[FA]} \qquad \text{(Eqn. 1)}$$

The inhibition constant ($K_{i,4-VG}$) was determined to be 0.14 mM which is in the same order of magnitude as the one reported by Jung *et al.*[30] Since a biotransformation characterized by a K_i/K_M ratio <1 would not proceed efficiently to complete conversion,[40] product inhibition by 4-VG constitutes a major problem for our approach ($K_{i,4-VG}/K_{M,FA}$ of 0.06). To validate the kinetic model, we compared the experimental data with the numerical solutions of the mass balance equations Eqn. 2.1 and 2.2 (Figure 1 and ESI Figure S6). k_d is the deactivation constant for the enzyme (k_d = 6.3×10^{-4} ± 1×10^{-4} min^{-1}, see details below).

$$-\frac{d[FA]}{dt} = [PAD]e^{-k_d t}\,v \qquad \text{(Eqn. 2.1)}$$

$$\frac{d[VG]}{dt} = [PAD]e^{-k_d t}\,v \qquad \text{(Eqn. 2.2)}$$

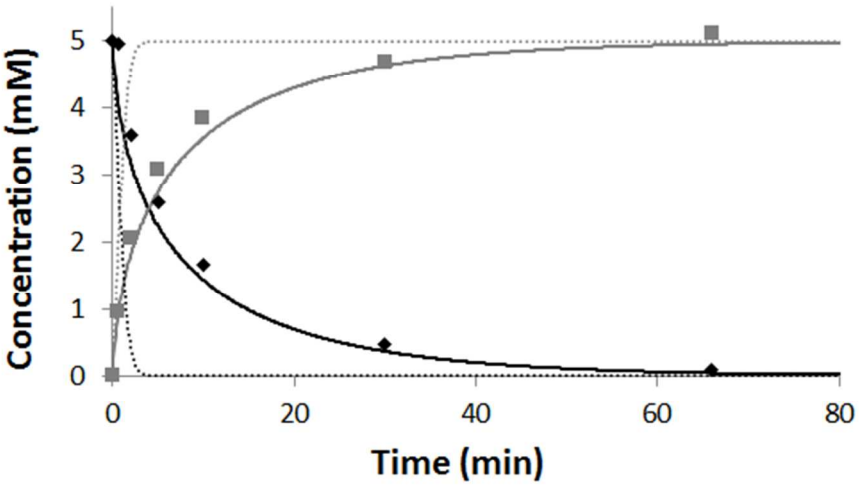

Figure 1. Comparison of experimental data (black diamonds: FA; grey squares: 4-VG) with the simulation of the kinetic model (continuous lines). Dotted lines represent the kinetic model without competitive product inhibition. Reaction conditions: 5 mM FA, 3.8 U mL^{-1} PAD (59 µg mL^{-1}) *Mc*PAD in KP_i buffer (0.1 M, pH 7.0) at 37°C at 700 rpm.

Figure 1 shows good agreement of the experimental with simulated data (black and grey continuous lines) and the significant effect of the product inhibition (black and grey dotted lines). Next, we analyzed the effect of substrate concentration on the maximum conversion (Figure 2) and the deviation from the theoretical data derived by the kinetic model.

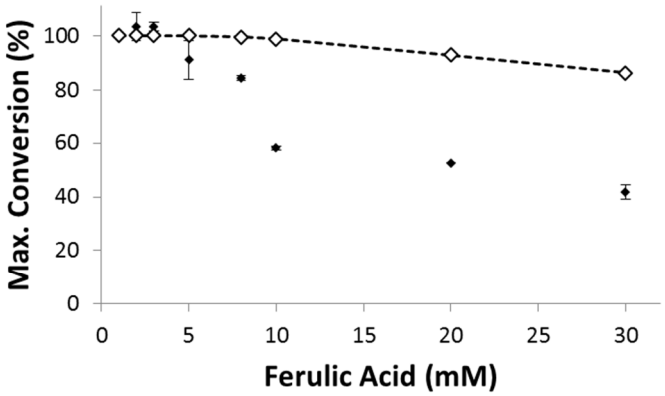

Figure 2. Influence of the substrate concentration on maximum conversion. Black diamonds: maximum conversion; white diamonds: theoretical maximum conversion according to Eqn.1 at 24 h. Reaction conditions: 1–30 mM FA, 0.5 U mL^{-1} (8 µg mL^{-1}) *Mc*PAD, in KP_i buffer (0.1 M, pH 7.0) at 37°C at 700 rpm. Standard deviations in duplicates 0.2–12%.

Such a trend does not derive from excess substrate inhibition (i.e. additional substrate binds to the enzyme-substrate complex), but is most likely due to enzyme deactivation at high product concentrations. In that respect, the maximal conversion should be dependent on the catalyst amount as observed in our results (ESI Figure S7). Data supporting this observation were also reported by Leisch and co-workers.[32]

To further study the influence of enzyme/substrate ratio on the maximal conversion, we evaluated the enzyme deactivation by comparing reaction progress curves at different biocatalyst concentrations. In the absence of deactivation, conversion *versus* time × PAD concentration data points should fall on the same line.[41,42] Our experiments show that this holds true at 5 mM FA but not at 10 mM, where different enzyme concentrations generate different progress curves at the late stage of the reaction (ESI Figure S8). Hence, the Eqn. 1 for this reaction system seems to be valid at high ferulic acid concentrations only when the enzyme concentrations are high enough [PAD (µg mL^{-1})/FA (mM) ratio ≈ 6]. Inhibition or deactivation of PADs by the reaction products have not been described in detail so far. Our data show an influence of 4-VG concentration on the enzyme, which could be exerted either by (irreversible) deactivation or by the establishment of a different inhibition type. From a practical point of view, to achieve high conversions in this system, as a rule of thumb the concentration of the product should be maintained below 10 mM when PAD concentration is <1.3 U mL^{-1}.

Two-Liquid Phase System (2LPS)

In order to increase the starting FA concentration, we investigated the possibility to use a 2LPS, where the organic phase would continuously remove the product from the aqueous phase, thereby keeping it under its inhibition threshold. Since the stability of PADs is an issue in the presence of organic solvents,[43,33,30] a trade-off between partition coefficients[33b] of the product and enzyme activity/stability needs to be made. Figure 3 shows the partition coefficients Kp (expressed as logarithm) and the reaction rate for extraction of 5 mM 4-VG while using solvents with $logP$ (1-octanol/water partition coefficient) values of 0.7–4.

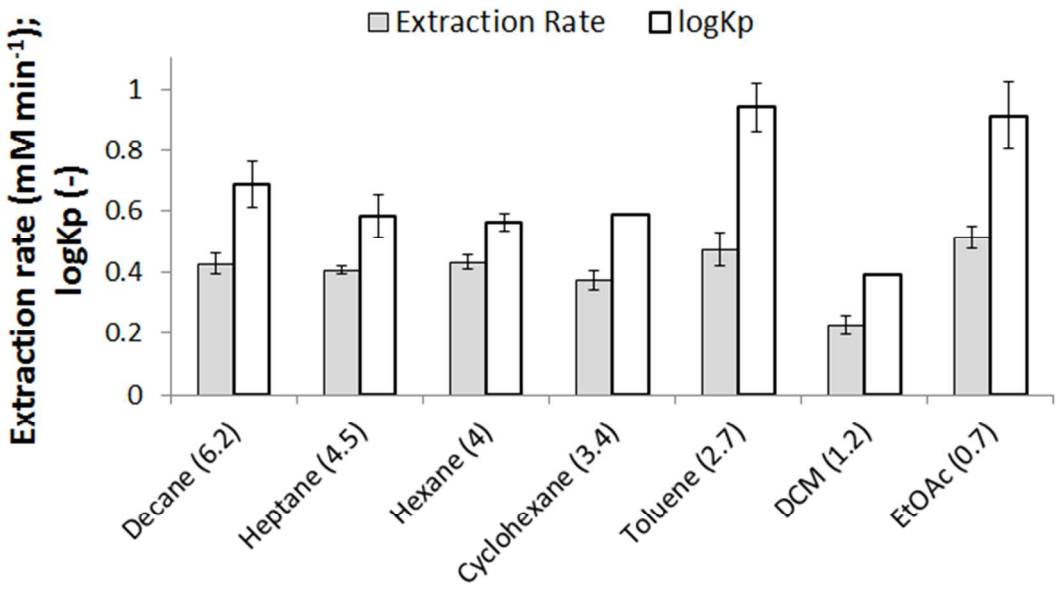

Figure 3. Extraction rates and partition coefficients of 4-VG in buffer:organic solvent systems. The $logP$ of each solvent is indicated in brackets. 5 mM 4-VG, 1:1 solvent ratio (v/v). Equilibrium was reached in all cases after approx. 1 h. DCM: dichloromethane, EtOAc: ethyl acetate. Standard deviations in duplicates 0.1–12% ($logKp$) and 3–12% (extraction rate).

The highest partition was observed for toluene and EtOAc, while the differences in extraction rates are not as significant. Biotransformations were first tested in small scale using 5 mM FA to verify whether the *Mc*PAD was compatible (Table 1).

Table 1. *Mc*PAD-catalyzed conversion of FA in two-liquid phase system using different organic solvents.

Solvent	Solubility in water[a]	$logP$	Conversion (%)
Hexane	<0.1	4	99
Toluene	<0.1	2.7	99
DCM	1.3	1.2	99
EtOAc	8.7	0.7	5

[a] g in 100 mL, 20°C. Reaction conditions: 5 mM FA, 0.78 U mL^{-1} (12 μg mL^{-1}) *Mc*PAD, in a 2LPS [aqueous: organic, 1:1 (v/v)], aqueous 0.1 M KP_i buffer at pH 7 and 37°C, 700 rpm. In the case of DCM, the organic phase is the lower phase, whereas in all other 2LPSs the organic phase is the upper phase.

The reaction runs to completion in hexane, toluene and DCM but not in EtOAc, due to its higher polarity and water solubility, leading to enzyme deactivation. We then selected hexane, toluene and DCM for further studies. Experiments performed with 20 mM FA and 8 μg mL^{-1} enzyme concentration using either hexane or toluene as the second phase showed already a consistent

improvement with respect to the reaction performed in buffer, as quantitative conversion was obtained after <10 h. The 4-VG concentration in buffer remained <4 mM (ESI Figure S9). The reaction rate in the 2LPS was 69% of the rate observed in the one-phase system. The organic phases contained only the target product allowing straightforward work-up to afford 4-VG. However, in the case of toluene, the product was isolated as a yellow oil (ESI Figure S10), indicating low purity. This fact has also been observed by Leisch et al.[32] Using hexane, 4-VG could be isolated in <70% yield as transparent oil. The maximum conversion in the presence of DCM was ~75%, probably due to enzyme deactivation by longer exposure to the organic phase. In addition, due to its higher density than water (DCM appears as lower phase) and low boiling point (40 °C), DCM is not an appropriate solvent in a 2LPS. Hence, hexane was chosen as a model solvent for further optimization studies. Enzyme stability in the presence of organic solvents is a critical factor for solvent choice and we therefore studied the stability of *Mc*PAD in a buffer/hexane system. Surprisingly, an increased stability of the enzyme (>3-fold) in the presence of hexane was detected (Figure 4).

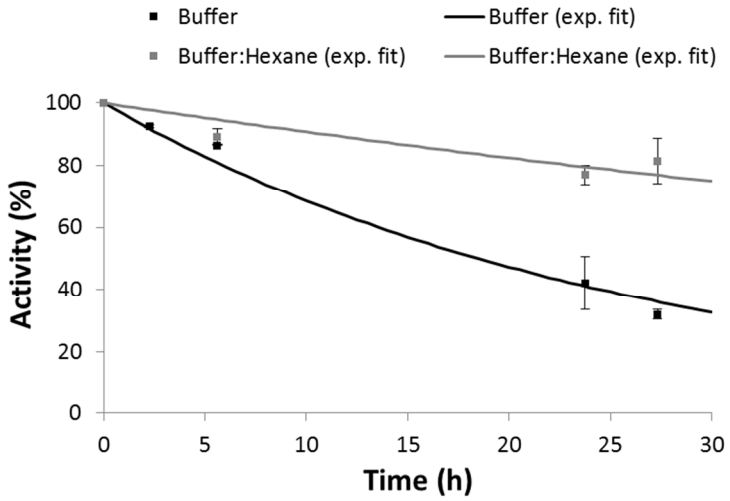

Figure 4. Stability of *Mc*PAD in buffer and buffer:hexane. Continuous black and grey lines represent an exponential fit to the experimental data. Reaction conditions: 5 mM FA, 0.39 U mL^{-1} (6 µg mL^{-1}) *Mc*PAD; in a 2LPS (aqueous:organic, 1:2 (v/v)), aqueous medium 0.1 M KP_i buffer at pH 7 and 37°C, 700 rpm. $t_{1/2}$ of *Mc*PAD in buffer = 15 h; $t_{1/2}$ of *Mc*PAD in buffer:hexane = 53 h. Standard deviations in duplicates 0.6–20% in buffer; 3–9% in buffer:hexane.

Decreased activity and increased stability in a 2LPS suggest the establishment of a rigid *Mc*PAD conformation. More flexible conformations facilitate substrate-enzyme interactions but at the same time decrease the thermostability.[44,45] Such flexibility changes may occur either at the interphase or by direct action of solubilized solvent molecules. In fact, even though the solubility of hexane in water is very low, this would result in a hexane/PAD concentration ratio of approx. 20–30 (depending on the enzyme loading).

Although half-life times in 2LPSs have not been reported so far, the stability of *Mc*PAD ($t_{1/2}$ of 53 h) seems to be superior to other PADs in a 2LPS.[30] It is worth mentioning that the PAD from (solvent tolerant) *B. licheniformis* CGMCC 7172 showed a remarkable stability towards high $logP$ organic solvents after 12 h of incubation.[33]

The construction of a kinetic model would allow a better understanding of the reaction and the *in silico* planning of further improvements of the reaction for technical-scale applications. Assuming no changes in the catalytic mechanism, we introduced in the mass balance the reversible extraction of the product in the organic phase (Eqn. 3.1 and 3.2).

$$v_1 = v - k_1[4-VG]_{aq} + k_{-1}[4-VG]_o \qquad \text{(Eqn. 3.1)}$$

$$v_{-1} = k_{1}[4-VG]_{aq} - k_{-1}[4-VG]_{o} \quad \text{(Eqn. 3.2)}$$

Where $[4\text{-VG}]_{aq}$ and $[4\text{-VG}]_{o}$ are the product concentrations in aqueous and organic phase, v_1 is the velocity for 4-VG formation in the aqueous phase, v is the velocity in Eqn.1, k_1 is the rate constant for the extraction into the organic phase and k_{-1} is the rate constant for the reverse direction; v_{-1} is the velocity of 4-VG extraction in the organic phase. The two constants k_1 and k_{-1} were estimated measuring extraction velocities in 5 mL thermostated vessels using 1 mL buffer and 2 mL hexane at two different 4-VG concentrations. k_1 = 0.097 min^{-1} and k_{-1}= 0.0078 min^{-1} (calculated dividing k_1 by the partition coefficient measured using an aqueous:organic ratio of 1:2 (v/v) ($logKp$ = 1.082). Since the catalytic constants of the enzyme would change in the presence of the second phase, we realized a fit of the proposed mass balance (using the deactivation constant for the enzyme k_d =1.6 × 10^{-4} ± 7.9 × 10^{-5} min^{-1}) to the reaction progress. The results show that this is a realistic model for the reaction (Figure 5 and ESI Figure S11). Table S1 shows the determined parameters.

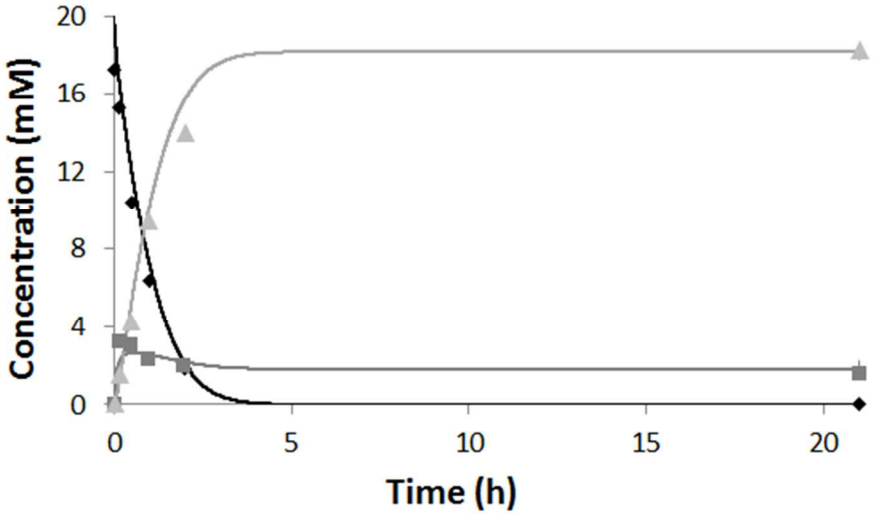

Figure 5. Comparison of experimental data with the kinetic model (continuous lines). Black diamonds: FA; grey squares: 4-VG in buffer, light grey triangles: 4-VG in hexane. Reaction conditions: 20 mM FA, 0.58 U mL^{-1} (9 μg mL^{-1}) *Mc*PAD, in a 2LPS [aqueous:organic, 1:2 (v/v)], aqueous medium 0.1 M KP_i buffer at pH 7 and 37°C, 700 rpm.

Figure 5 shows a typical reaction progress in the 2LPS, where the product accumulates in the aqueous medium reaching a maximum and the extraction into the organic phase continues up to an equilibrium point. Initial attempts to run the reaction at 50–100 mM failed because of the pH increase to 8.0 during the course of the reaction. In order to solubilize FA in KP_i buffer (0.1 M, pH 7.0) KOH was added (final concentration 70 mM), and as the acid substrate is converted, the pH would become increasingly alkaline and hence buffer capacity (especially at high FA concentrations) plays a major role in the productivity of the enzyme. Table 2 shows that the increase in the buffer concentration significantly improved the conversions.

Table 2. Influence of the ferulic acid concentration and buffer strength on the maximum conversion.

Ferulic Acid (FA) Concentration (mM)	KP_i Buffer Concentration (M)	Max. Conversion (%)
100	0.1	41
50	0.1	66

50	0.5	99
100	0.5	95
200	0.5	30
200	0.1 [a]	60
120	0.5	87

[a] Reaction operated with pH control and autotitrator. Reaction conditions: 50–200 mM FA, 0.84 U mL^{-1} (13 µg mL^{-1}) *Mc*PAD, in a 2LPS (aqueous:organic, 1:2 (v/v)), aqueous medium KP_i buffer at pH 7 and 37°C, 700 rpm.

The results show that with sufficient buffer capacity, the reaction can proceed to high conversions (87%) up to 120 mM. Beyond 200 mM, even with continuous pH titration, inhibitory product concentrations in the aqueous phase are dominant. Table 3 shows the process parameters for the optimized reaction at 100 mM FA.

Table 3. Process parameters for the optimized reaction conditions at 100 mM (19 g L^{-1}) ferulic acid (FA).

FA	PAD	X	Y	TON	EC

($g\ L^{-1}$)	($mg\ mL^{-1}$)/($U\ mL^{-1}$)	(%)	(%)	($mol\ mol^{-1}$)	($kg\ g^{-1}$)
19	0.09/5.8	95	79	11734	89

X = Conversion; Y = Isolated yield; TON = Turnover number (maximum conversion at 23 h); EC = Enzyme consumption (kg product/g of enzyme). Optimized reaction conditions: 100 mM (19 g L^{-1}) FA, 5.8 U mL^{-1} (0.09 mg mL^{-1}) *Mc*PAD, in a 2LPS (aqueous:hexane, 1:2 (v/v), 10 mL:20 mL), aqueous medium 500 mM KPi buffer at pH 7 and 37°C, 700 rpm.

At this concentration, the reaction progress can be simulated in good agreement only during the first 2 h of the reaction (Figure S11-C), afterwards it proceeded slower than expected. A possible reason can be the presence of product concentrations >10 mM in the aqueous phase, causing enzyme deactivation or product inhibition as mentioned above. The reaction was demonstrated also at gram scale (1.9 g FA) in 100 mL reaction volume, which afforded 1 g of 4-VG with 89% conversion and 75% isolated yield.

A limitation of this system is caused by the partition coefficient of 4-VG, which generates a steady-state product concentration in the aqueous phase of about 2 mM and which limits the use of higher FA concentrations. These problems could be circumvented by using higher organic solvent volumes. We addressed these issues by designing a recycling system that allowed to reduce the amount of hexane, while at the same time facilitated product isolation. The system is presented in Scheme 3 and a photograph of the set-up is shown in the ESI, Figure S12.

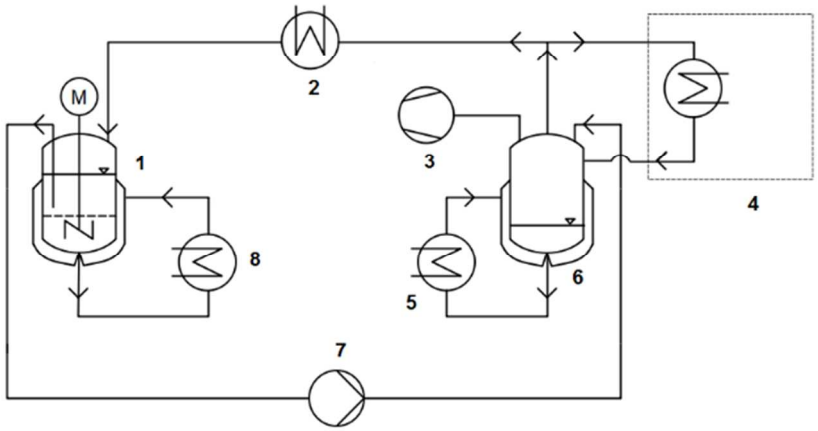

Scheme 3. Flow scheme of the extraction/distillation reactor set-up. 1: two-phase reactor; 2: distillation condenser (4°C); 3: vacuum pump connected with the distillation system (400–450 mbar); 4: bubble condenser (4°C); 5: thermostat (50–55°C); 6: vessel collecting product solution; 7: tube pump (0.25 mL min^{-1}); 8: thermostat (37°C).

In this reactor set-up, the organic phase containing the product is continuously pumped (7) into a second reactor (6) where hexane is distilled under vacuum to re-enter the two-phase reactor (1), while 4-VG (Bp. 220°C) accumulates in the distillation vessel (6). Figure 6 compares the reaction in the standard set-up and in the reactor set-up depicted in Scheme 3. Using the integrated recycling system, quantitative conversions were achieved in shorter time with complete product extraction from the aqueous phase. This set-up was also successfully used at 170 mM substrate concentration (with 92% conversion). Moreover, since at such high FA concentrations a continuous autotitration system (3 M HCl) is necessary, the reaction was performed in unbuffered distilled water, thereby reducing the input material (Table 4).

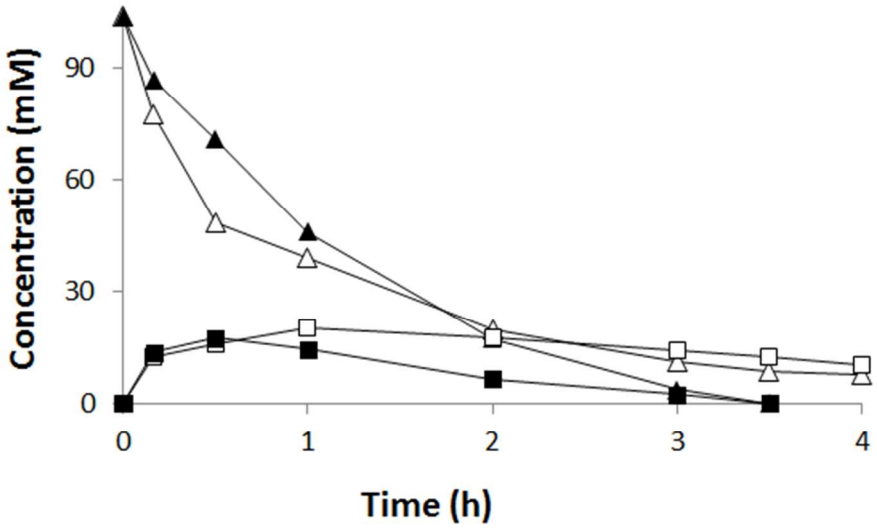

Figure 6. Decarboxylation of FA in 2LPS (FA: white triangles; 4-VG: white squares) and in the extraction-distillation apparatus (FA: black triangles; 4-VG: black squares). Reaction conditions: 100 mM FA, 3.9 U mL^{-1} (60 µg mL^{-1}) *Mc*PAD, in a 2LPS [aqueous:hexane, 1:2 (v/v)], aqueous medium 0.1 M KP_i buffer at pH 7 and 37°C, 700 rpm.

Table 4. Comparison of reactor set-ups involving distillation.

FA Conc. (mM)	FA Conc. (g L^{-1})	Conditions	Conversion (%)
100	19.4	Extract./distill.	>99
200[a]	38.8	0.1 M KP_i Buffer, pH 7	60
170	33	Extract./distill.[b]	92

[a] Data from Table 2 inserted as comparison.

[b] Reactions operated in distilled water with pH control and autotitrator.

Chemical Reduction of 4-VG to 4-EG

The hydrogenation of 4-VG was attempted at 2 mL scale using the homogeneous Wilkinson catalyst [$RhCl(PPh_3)_3$] and heterogeneous Pd on C. The use of 10 mol% Wilkinson catalyst afforded low conversion (<10%) after 1 h at room temperature and the reaction did not proceed further. Temperature increase up to 40°C and solvent change (toluene, methanol, dichloromethane) did not improve the reaction performance. These results indicate catalyst inhibition/deactivation by the substrate, possibly *via* coordination of the phenolic group. Pd on C, on the other hand, was very efficient (Scheme 4).

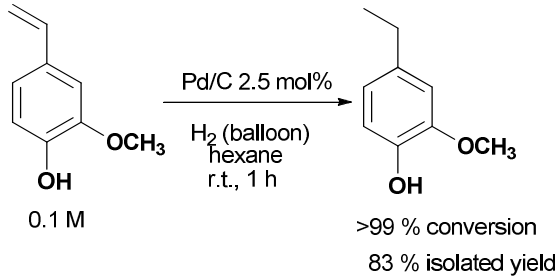

Scheme 4. Hydrogenation of 4-VG to 4-EG using Pd/C as catalyst.

The reaction afforded the expected product 4-EG with complete selectivity in 83% isolated yield after a simple filtration of the catalyst and solvent evaporation.

PAD–Pd/C Reaction Sequence to 4-EG

The complete two-step PAD-Pd/C sequence was performed on a gram scale (1.94 g FA, 100 mL volume), where after the biocatalytic reaction the organic layer was withdrawn with a syringe

and transferred into the reactor containing the metal catalyst. An isolated yield of 70% for the final product 4-EG (1.1 g) was achieved. The identity of both products was verified by TLC and HPLC by comparison with commercial reference materials, and by GC-MS (ESI Figure S13). The performances of both steps in terms of reaction rates and conversion show that the bottleneck of the whole system is the enzymatic step, which needed further optimization in view of substrate concentration, biocatalyst loading and reaction conditions.

Use of Alternative Organic Solvents

Hexane was chosen as solvent because of the satisfactory performance in view of conversion, enzyme stability, product purity and low boiling point allowing faster product isolation. However, it has recently been classified as a non-desirable solvent.[46] For this reason we investigated alternative solvents (ESI Table S2), such as MTBE (methyl *tert*-butyl ether), 2-methyl-THF (2-MeTHF) and heptane. The reaction proceeded smoothly to 96% conversion at 5 mM FA using MTBE as the second phase but only to 45% at 100 mM. 2-MeTHF caused instantaneous enzyme deactivation, comparable to EtOAc (ESI Table S2). Heptane seems to be the best alternative, as the reaction performed equally well as in hexane. In general, solvents with $logP$ below ~1 and water solubility >2 g in 100 mL were found to be detrimental to the enzyme. This behavior can be related to the stripping of essential water molecules by hydrophilic solvents.[47]

Analysis of the Environmental Impact

The E-factor ($kg_{waste}/kg_{product}$) is a simple indicative estimation of the environmental impact of a synthetic procedure,[48] which allows to quantitatively compare methodologies at the early stages of development and to pinpoint improvements. According to Scheme 1, environmental analysis

for 4-VG synthesis was realized for routes 3, 4 and 5 (base-catalyzed decarboxylation). E-Factors were calculated separately for the reaction (ESI Figure S14) and for product isolation (ESI Figure S15-A), solvents were addressed separately and expressed as solvent demand (mL solvent/g of product, ESI Figure S15-B).

The chemical (AcOH-catalyzed at ΔT) and biocatalytic routes from FA appear comparable, the advantage of the enzymatic route becomes clear when considering the E-factor for work-up and isolation (ESI Figure S15-A), which causes a 150-fold increase in the heat/AcOH decarboxylation. However, the reaction's solvent demand for the enzymatic route is highest (ESI Figure S15-B). Sub-molar reactant concentrations in enzymatic reactions are a preponderant cause of high E-factors.[49] However, considering both reaction and workup together, the biocatalytic route has the second lowest value among the seven routes (ESI Figure S15-B).

The synthesis of 4-EG in the two-step sequence was compared with route 2 and 3 (*via* stoichiometric Clemmensen reduction versus the catalytic variant and the Wittig/hydrogenation sequence). The alkylation route is difficult to compare because of unavailability of data, especially its selectivity, and because these reactions are normally conducted in the gas phase in continuous flow. Figure S16 shows the results in terms of E-factor for the reaction. The superiority of the catalytic routes is evident.

Due to the relatively low concentration of the starting material in the enzymatic reaction, the E-factor for work-up/isolation and the solvent demand are quite high. Such values are in fact direct consequences of the large volumes used (ESI Figure S17). Solvent recycling, as shown in Figure 4 is clearly an appealing solution to decrease the overall solvent load substantially. In addition to that, high substrate concentrations would lower the E-factor as well.

CONCLUSIONS

A two-step synthetic sequence to the fragrance compound 4-ethylguaiacol (4-EG) starting from ferulic acid was investigated and established. The route involved the decarboxylation of ferulic acid catalyzed by a phenolic acid decarboxylase from *Mycobacterium colombiense*, yielding 4-vinylguaiacol (4-VG) followed by hydrogenation to 4-EG by Pd/C, without intermediate isolation. Careful optimization was required regarding the enzymatic step to overcome constraints in terms of product inhibition and deactivation.

Without continuous product removal, the PAD-catalyzed decarboxylation of FA was demonstrated at gram scale (100 mM, 19 g L^{-1}) resulting in 89% conversion and 75% isolated yield. However, a reactor strategy integrating product isolation afforded 92% conversion of 170 mM (33 g L^{-1}) FA to 4-VG. Drawbacks of this reactor set-up are, however, the higher complexity and energy input. The complete sequence (PAD–Pd/C) was demonstrated at gram scale, resulting in 4-EG (1.1 g) with 70% overall isolated yield in a two steps-two pots process. The environmental feasibility of these synthetic steps was estimated, which favourably compared with other approaches. Enzyme screening/optimization in terms of activity and stability in connection with reaction engineering makes the whole system appealing for technical applications. Expanding of the scope of the chemo-enzymatic approach by using alternative carboxylic acids (e.g. coumaric acid, sinapic acid, caffeic acid) is ongoing in our laboratories.

EXPERIMENTAL SECTION

Materials. Ferulic acid was purchased from Carl Roth (Germany), all the other chemicals were purchased from Sigma Aldrich (Buchs, Switzerland). For preparative experiments, hexane was degassed using nitrogen prior to use. Data were acquired using HPLC with UV detection using

calibration curves obtained with authentic reference materials. Mathematical regressions to algebraic equations were performed using Microsoft Excel® (Excel 2010, Microsoft). Mathematical regressions to differential equations and numerical solutions of differential equations were performed using the ODE45 solver implemented in Matlab® (Matlab 2010, Mathworks). Docking simulations were realized with Autodock 4.0 and the estimation of the environmental impact was partly performed using EATOS (Environmental Assessment Tool for Organic Syntheses).

Enzyme Production and Purification. *E. coli* BL21 (DE3) cells were transformed with the plasmid pET21a(+) containing the His-tagged *Mc*PAD decarboxylase gene and heterologous expression was performed as previously reported.[50] To prepare cell-free extracts (CFEs), wet cells (4 g mL^{-1}) were suspended in potassium phosphate (KP_i) buffer (0.05 M, pH 7.0) and the suspension was sonicated (5 mm sonication tip, 70 % power, 50% duty cycle, 3 min) on ice for three times and centrifuged at 24000 rpm (69673 rcf) for 20 min at 4°C.

Enzyme purification was carried out using a Nickel-NTA-agarose packed column (9 cm high, conical 0.8 x 4 cm). After washing the column with an equilibration buffer (Tris 20 mM, NaCl 300 mM, imidazole 10 mM, pH 7.4) with 3 column volumes, the CFE was loaded by gravity flow using a ratio of 0.4 mL of CFE mL^{-1} of the chromatographic matrix (corresponding to 10 mg total protein/mL of matrix). Unspecifically adsorbed proteins were removed by washing with 5 column volumes of washing buffer (Tris 20 mM, NaCl 300 mM, imidazole 20 mM, pH 7.4) and *Mc*PAD was eluted using 2.5 column volumes of elution buffer (Tris 20 mM, NaCl 300 mM, imidazole 250 mM, pH 7.4). Protein adsorption was carried out at 4°C, all the other steps were carried out at room temperature. Imidazole was removed by centrifugation (5000 rpm (3850 rcf)

for 10 min at 4°C) using membrane-tubes (10 KDa cut-off) using an exchange buffer (KP_i buffer, 50 mM, pH 7.0) for storage. Obtained CFEs were stored at -20°C.

Activity Assays. Activity data were acquired *via* direct initial rate measurements using HPLC equipped with an UV detection system. Unless otherwise stated, for screening experiments and kinetic constant determinations, assays were performed in KP_i buffer 0.1 M, pH 7.0 in glass vials (1 mL volume) shaken at 700 rpm. After addition of the appropriate buffer and substrate, the reaction was started by addition of the enzyme. Samples (50 µL) were withdrawn and diluted with a water:acetonitrile solution (20:80 + 3% v/v trifluoroacetic acid) to stop the reaction. The samples were centrifuged (5 min, 13000 rpm/15700 rcf) and analyzed by HPLC. Using the fermentation protocol and the CFE preparation method described above, 10–20 µL of extract (corresponding to 0.2–0.5 mg mL^{-1} total protein in the assay) are appropriate to detect the linear range (<10 % conversion) within a 3 min. interval. U mL^{-1} values reported for each experiment refer to a reference assay performed in 1 mL volume (HPLC glass vials) using KP_i buffer 0.1 M pH 7.0, 5 mM FA, shaking with 700 rpm at 37°C. Apart from the kinetic measurements, reactions were performed using CFEs. Enzyme concentrations given in the manuscript represent the target enzyme in the CFE.

Determination of Partition Coefficients and Extraction Rates. Partition coefficients were calculated following extraction progress curves of 5 mM 4-VG in buffer/organic solvents mixtures (1:1) in 1 mL volume in glass HPLC vials at 37 °C and 700 rpm. The ratios of the concentration in organic/aqueous phase were calculated at equilibrium, which was reached after ~1 hour. Extraction rates were calculated by fitting the concentration increase in the organic phase to an exponential function.

Decarboxylation of FA in a 2LPS. The optimized reaction conditions at 100 mM FA concentration are described here as an example: 194 mg (1 mmol) of ferulic acid were added to a 50 mL thermostated vessel equipped with a magnetic stir bar. After addition of 7 mL of an aqueous solution composed of KPi buffer (0.5 M, pH 7.0) and 70 mM KOH, the mixture was stirred vigorously at 37°C until FA was completely solubilized. After the addition of 20 mL of hexane, the reaction was started by the addition of enzyme solution (3 mL, 90 μg mL^{-1} final concentration) to the aqueous layer and stirred at 37°C and 500 rpm. After the reaction was complete, the organic layer was separated, dried ($MgSO_4$), filtered and evaporated, yielding 118 mg (79% yield) of 4-VG as transparent oil. The identity of the product was assayed comparing analytical data with the commercial reference material. TLC (R_f = 0.7 in hexane:EtOAc 2:1); GC-MS: m/z = 150 [M^+], 135 [$C_8H_7O_2^+$], 107 [$C_7H_7O^+$], 77 [$C_6H_5^+$].

Synthesis of 4-EG. 100 mM 4-VG in hexane was transferred *via* syringe and under nitrogen flow into a two-neck reactor previously charged with Pd/C (2.5 mol%, 5 % Pd basis) and connected to a hydrogen balloon. After three vacuum (2 mbar)-nitrogen cycles, the reaction was started by the establishment of a hydrogen atmosphere inside the reactor and was carried out for 1 h at room temperature under vigorous stirring. After the reaction was complete, the mixture was filtered through Celite® under nitrogen gas and the solvent was evaporated to yield a transparent oil in 80% yield. In the synthesis starting from ferulic acid, the organic layer from the decarboxylation reactor was transferred to the hydrogenation reactor following the same steps as mentioned before. The identity of the product was assayed comparing analytical data with commercial reference material. TLC (R_f= 0.8 in hexane:EtOAc 2:1); GC-MS: m/z = 152 [M^+], 137 [$C_8H_9O_2^+$], 91 [$C_7H_7^+$], 77 [$C_6H_5^+$].

Analytical Methods. The reaction components FA, 4-VG and 4-EG were analyzed by an Agilent LC-1100 HPLC equipped with a diode array detector using a LiChroCART® 250-4 LiChrospher 100 RP-18 5 µm column, at 25°C. As mobile phases, water/trifluoroacetic acid (0.1 %) and acetonitrile/trifluoroacetic acid (0.1 %) with a flow rate of 1 mL min^{-1} with a gradient (0–2 min 15% acetonitrile; 2–10 min 15–100%; 10–12 min 100–15%) were used. FA and 4-EG were detected at 280 nm, whereas 4-VG was detected at 254 nm. Typical retention times were 7.8 min for FA, 9.8 min for 4-VG and 10.1 min for 4-EG. Calibration curves were set up using commercial reference materials. 4-VG and 4-EG were analyzed by an Agilent 7890A GC using a HP-5 (30 m x 320 µm, 0.25 µm) column coupled to an Agilent 5975C quadrupole mass spectrometer. Method: 80°C for 1 min, 5°C min^{-1} to 235°C for 34 min (He 1.5 mL min^{-1}). Retention times for 4-VG and 4-EG were 6.75 and 7.78 min, respectively.

Estimation of the Environmental Factor (E-Factor). E-factors were calculated with the aid of the free-ware software EATOS (Environmental Assessment Tool for Organic Syntheses). When not specified by the procedure, the following values were assumed: desiccant: 20 g L^{-1} of solution; Celite® for filtration: 0.1 g mL^{-1} of solution; silica gel for chromatography: 20 g g^{-1} of product; eluents for chromatography: 500 mL g^{-1} of product. ‡

ASSOCIATED CONTENT

Supporting Information Available

Details on the characterization of the enzyme, use of alternative organic solvents, experimental set-up, E-factor analysis.

AUTHOR INFORMATION

Corresponding Authors

*Tel.: (+49) 040 42878 3018 (A. Liese), (+49) 040 42878 2890 (S. Kara), Fax: (+49) 040 42878 2127, E-mail: liese@tuhh.de; selin.kara@tuhh.de

Author Contributions

The manuscript was written through contributions of all authors. All authors have given approval to the final version of the manuscript.

Notes

‡ Additional information about the assumptions made is presented in the Supporting Information.

The authors declare no competing financial interest.

ACKNOWLEDGMENT

The authors gratefully acknowledge Dr. Joerg H. Schrittwieser (Department of Chemistry, University of Graz) for proofreading the manuscript.

ABBREVIATIONS

PAD, phenolic acid decarboxylases; *Mc*PAD, PAD from *Mycobacterium colombiense*; 4-VG, 4-vinylguaiacol; 4-EG, 4-ethylguaiacol; Pd/C, palladium on charcoal.

REFERENCES

1 P.N.R. Vennestrøm, C. H. Christensen, S. Pedersen, J.-D. Grunwaldt and J. M. Woodley, *ChemCatChem*, 2010, 2, 249–258.

2 S. K. Karmee, C. Roosen, C. Kohlmann, S. Lütz, L. Greiner and W. Leitner, *Green Chem.*, 2009, 11, 1052–1055.

3 R. C. Simon, C. S. Fuchs, H. Lechner, F. Zepeck and W. Kroutil, *Eur. J. Org. Chem.*, 2013, 2013, 3397–3402.

4 J. H. Schrittwieser, F. Coccia, S. Kara, B. Grischek, W. Kroutil, N. d'Alessandro and F. Hollmann, *Green Chem.*, 2013, 15, 3318–3331.

5 O. Långvik, T. Sandberg, J. Wärnå, D. Y. Murzin and R. Leino, *Catal. Sci. Technol.*, 2015, 5, 150–160.

6 A. L. Flourat, Peru, A. A. M., Teixeira, A. R. S., F. Brunissen and F. Allais, *Green Chem.*, 2015, 17, 404–412.

7 F. Shahidi and M. Naczk, *Phenolics in food and nutraceuticals*, CRC Press, Boca Raton, 2003.

8 G. A. Burdock, *Fenaroli´s Handbook of Flavor Ingredients, 6th Edition*, CRC Press, Boca Raton, 6th edn., 2010.

9 G. D. Yadav and G. S. Pathre, *Ind. Eng. Chem. Res.*, 2007, 46, 3119–3127.

10 S. K. Chittimalla, C. Bandi, S. Putturu, R. Kuppusamy, K. C. Boellaard, Tan, David Chu Aan and Lum, Demi Ming Jie, *Eur. J. Org. Chem.*, 2014, 2014, 2565–2575.

11 L. Petitjean, R. Gagne, E. S. Beach, D. Xiao and P. T. Anastas, *Green Chem.*, 2016, 18, 150–156.

12 C. J. Simpson, M. J. Fitzhenry, N. Patrick, J. Stamford, *Tetrahedron Lett.*, 2005, 46, 6893–6896.

13 V. Aldabalde, *OJPC*, 2011, 1, 85–93.

14 M. J. Rein, V. Ollilainen, M. Vahermo, J. Yli-Kauhaluoma and M. Heinonen, *Eur. Food Res. Technol.*, 2005, 220, 239–244.

15 C. R. Smith, T. V. RajanBabu, *Tetrahedron*, 2010, 30, 1102–1110.

16 N. A. Bumagin and E. V. Luzikova, *J. Organomet. Chem.*, 1997, 532, 271–273.

17 A. F. Littke, L. Schwarz and G. C. Fu, *J. Am. Chem. Soc.*, 2002, 124, 6343–6348.

18 US patent 2005/0228191 A1, 2005.

19 R. Bernini, E. Mincione, M. Barontini, G. Provenzano and L. Setti, *Tetrahedron*, 2007, 63, 9663–9667.

20 A. Sharma, R. Kumar, N. Sharma, V. Kumar and A. K. Sinha, *Adv. Synth. Catal.*, 2008, 350, 2910–2920.

21 N. Kumar and V. Pruthi, *Biotechnol. Rep.*, 2014, 4, 86–93.

22 J. P. N. Rosazza, Z. Huang, L. Dostal, T. Volm, B. Rousseau, *J. Ind. Microbiol.*, 1995, 15, 457–471.

23 T. Hamada, M. Sugishita, H. Motai, *J. Ferment. Bioeng.*, 1990, 69, 166–169.

24 Y. Suezawa, M. Suzuki, *Biosci. Biotechnol. Biochem.*, 2007, 71, 1058–1062.

25 I. Baqueiro-Peña, G. Rodríguez-Serrano, E. González-Zamora, C. Augur, O. Loera and G. Saucedo-Castañeda, *Bioresour. Technol.*, 2010, 101, 4721–4724.

26 S. Y. Kang, O. Choi, J. K. Lee, J.-O. Ahn, J. S. Ahn, B. Y. Hwang and Y.-S. Hong, *Microb. Cell Fact.*, 2015, 14, 78.

27 I. Tchobanov, L. Gal, M. Guilloux-Benatier, F. Remize, T. Nardi, J. Guzzo, V. Serpaggi and H. Alexandre, *FEMS Microbiol. Lett.*, 2008, 284, 213–217.

28 A. Zago, G. Degrassi, C. V. Bruschi, *Appl. Environ. Microbiol.*, 1995, 61, 4484–4486.

29 J. Cavin, L. Barthelmebs, J. Guzzo, J. Van Beeumen, B. Samyn, J. Travers, C. Diviès, *FEMS Microbiol. Lett.*, 1997, 147, 291–295.

30 D. H. Jung, W. Choi, K.-Y. Choi, E. Jung, H. Yun, R. J. Kazlauskas and B.-G. Kim, *Appl. Microbiol. Biotechnol.*, 2013, 97, 1501–1511.

31 K. L. Morley, S. Grosse, H. Leisch and Lau, Peter C. K., *Green Chem.*, 2013, 15, 3312.

32 H. Leisch, S. Grosse, K. Morley, K. Abokitse, F. Perrin, J. Denault and P. C. Lau, *Green Process. Synth.*, 2013, 2, 7–17.

33 a) H. Hu, L. Li and S. Ding, *Appl. Microbiol. Biotechnol.*, 2015, 99, 5071–5081; b) G. P. Prpich, A. Daugulis, *Biotechnol. Bioeng.*, 2007, 97, 536–543.

34 H. Rodríguez, I. Angulo, de Las Rivas, Blanca, N. Campillo, J. A. Páez, R. Muñoz and J. M. Mancheño, *Proteins*, 2010, 78, 1662–1676.

35 J. M. Landete, H. Rodríguez, J. A. Curiel, de Las Rivas, Blanca, J. M. Mancheño and R. Muñoz, *J. Ind. Microbiol. Biotechnol.*, 2010, 37, 617–624.

36 M. W. Bhuiya, S. G. Lee, J. M. Jez and O. Yu, *Appl. Environ. Microbiol.*, 2015, 81, 4216–4223.

37 H. K. Huang, L. Chen, M. Tokashiki, T. Ozawa, T. Taira, S. Ito, *AMB Express*, 2012, 2, 1–10.

38 J. F. Cavin, V. Dartois, C. Divies, *Appl. Environ. Microbiol.*, 1998, 64, 1466–1471.

39 W. Gu, J. Yang, Z. Lou, L. Liang, Y. Sun, J. Huang, X. Li, Y. Cao, Z. Meng and K.-Q. Zhang, *PloS one*, 2011, 6, e16262.

40 (a) L. G. Lee, G. M. Whitesides, *J. Org. Chem.*, 1986, 51, 25–36; (b) A. Liese, M. Karutz, J. Kamphuis, C. Wandrey, U. Kragl, *Biotechnol. Bioeng.*, 1996, 51, 544–550.

41 M. J. Selwyn, *Biochim. Biophys. Acta*, 1965, 105, 193–195.

42 L. Pesci, S. M. Glueck, P. Gurikov, I. Smirnova, K. Faber and A. Liese, *FEBS J.*, 2015, 282, 1334–1345.

43 C. Wuensch, N. Schmidt, J. Gross, B. Grischek, S. M. Glueck and K. Faber, *J. Biotechnol.*, 2013, 168, 264–270.

44 A. M. Klibanov, *Nature*, 2001, 409, 241–246.

45 G. Carrea, S. Riva, *Angew. Chem. Int. Ed.*, 2000, 39, 2226–2254.

46 D. Prat, J. Hayler, A. Wells, *Green Chem.* 2014, 16, 4546–4551.

47 C. Laane, *Biocatalysis*, 1987, 1, 17–22.

48 R. A. Sheldon, *Chem. Commun.*, 2008, 3352–3356.

49 Y. Ni, D. Holtmann and F. Hollmann, *ChemCatChem*, 2014, 6, 930–943.

50 C. Wuensch, T. Pavkov-Keller, G. Steinkellner, J. Gross, M. Fuchs, A. Hromic, A. Lyskowski, K. Fauland, K. Gruber, S. M. Glueck and K. Faber, *Adv. Synth. Catal.*, 2015, 357, 1909–1918.

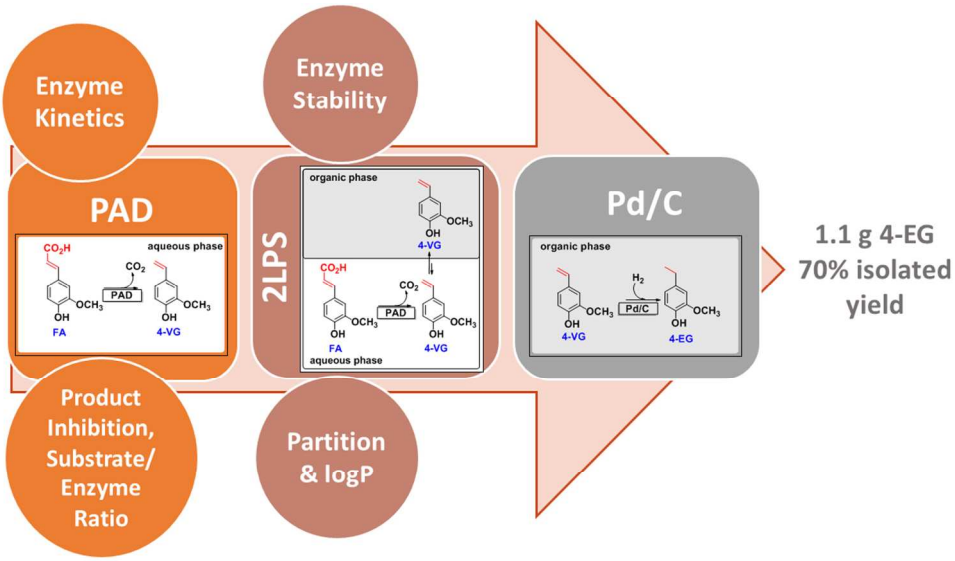

Table of Contents Graphic

338x190mm (96 x 96 DPI)